



CHORUS

This is the accepted manuscript made available via CHORUS. The article has been published as:

Finite-size critical scaling in Ising spin glasses in the mean-field regime

T. Aspelmeier, Helmut G. Katzgraber, Derek Larson, M. A. Moore, Matthew Wittmann, and Joonhyun Yeo

Phys. Rev. E **93**, 032123 — Published 14 March 2016

DOI: [10.1103/PhysRevE.93.032123](https://doi.org/10.1103/PhysRevE.93.032123)

Finite-size critical scaling in Ising spin glasses in the mean-field regime

T. Aspelmeier,^{1,2,3} Helmut G. Katzgraber,^{4,5,6} Derek Larson,⁷
M. A. Moore,⁸ Matthew Wittmann,⁷ and Joonhyun Yeo⁹

¹*Felix Bernstein Inst. Math. Stat. Biosci., Göttingen, Germany*

²*Univ. Göttingen, Inst. Math. Stochast., D-37073 Göttingen, Germany*

³*Max Planck Inst. Biophys. Chem., Stat. Inverse Problems Biophys. Grp., D-37077 Göttingen, Germany*

⁴*Department of Physics and Astronomy, Texas A&M University, College Station, Texas 77843-4242, USA*

⁵*Santa Fe Institute, 1399 Hyde Park Road, Santa Fe, New Mexico 87501 USA*

⁶*Applied Mathematics Research Centre, Coventry University, Coventry, CV1 5FB, England*

⁷*Department of Physics, University of California, Santa Cruz, California 95064, USA*

⁸*School of Physics and Astronomy, University of Manchester, Manchester M13 9PL, UK*

⁹*Division of Quantum Phases and Devices, School of Physics, Konkuk University, Seoul 143-701, Korea*

We study in Ising spin glasses the finite-size effects near the spin-glass transition in zero field and at the de Almeida-Thouless transition in a field by Monte Carlo methods and by analytical approximations. In zero field, the finite-size scaling function associated with the spin-glass susceptibility of the Sherrington-Kirkpatrick mean-field spin-glass model is of the same form as that of one-dimensional spin-glass models with power-law long-range interactions in the regime where they can be a proxy for the Edwards-Anderson short-range spin-glass model above the upper critical dimension. We also calculate a simple analytical approximation for the spin-glass susceptibility crossover function. The behavior of the spin-glass susceptibility near the de Almeida-Thouless transition line has also been studied, but here we have only been able to obtain analytically its behavior in the asymptotic limit above and below the transition. We have also simulated the one-dimensional system in a field in the non-mean-field regime to illustrate that when the Imry-Ma droplet length scale exceeds the system size one can then be erroneously lead to conclude that there is a de Almeida-Thouless transition even though it is absent.

PACS numbers: 75.10.Nr, 75.40.Cx, 05.50.+q, 75.50.Lk

I. INTRODUCTION

The nature of the ordered state of spin glasses remains controversial, despite decades of research. There are competing theories for the order parameter of the low-temperature phase. The oldest is based on the broken replica symmetry (RSB) theory of Parisi and co-workers [1–5], which gives the correct solution of the spin-glass problem in infinite space dimensions (mean-field regime), that is, for the Sherrington-Kirkpatrick (SK) model [6]. Alternative theories based on scaling arguments include the droplet model [7–11]. There are also theories based on rigorous calculations [12–17] which attempt to describe the behavior of these complex and poorly-understood systems, yet contradict the mean-field picture of Parisi. Recently, it has been argued that the RSB picture applies in space dimensions $d > 6$, while the droplet picture holds for $d \leq 6$ [18, 19]. That 6 might be the special dimension down to which RSB might be applicable has been rigorously established for a particular extreme choice of the spin-spin interactions [20].

The thrust of the argument brought forward in Ref. 18 concerns the phase transition which would take place in spin glasses in an external field if there were RSB—the so-called de Almeida-Thouless (AT) transition [21]. Furthermore, it was argued in Ref. 18 that when $d > 6$ the AT transition line is mean-field like so that $d_u = 6$ is the upper critical dimension. In renormalization group (RG) language this means its critical behavior is con-

trolled by a Gaussian fixed point. This point of view is supported by the work of Castellana and Barbieri [22], who obtained an equivalent result for a Dyson model on a hierarchical lattice. However, the arguments of Ref. 18 and 22 were based on *perturbative* results and it has been recently suggested [23] that there might be a new non-Gaussian fixed point controlling the behavior in a field in high space dimension. In addition, Castellana and Parisi [24] further suggested on the basis of a numerical study of the Dyson hierarchical model that a nonperturbative fixed point might also be controlling the critical regime in the parameter range which corresponds to $d \leq 6$. We decided therefore to reexamine previously-published Monte Carlo data in search of the nonperturbative fixed points. Based on our analysis, we conclude that at least for $d > 6$ there is strong evidence that the critical behavior both in a field and in zero field is controlled by the trivial Gaussian fixed point. In addition, in Sec. VI below we argue that finite-size effects will always make it difficult when $d \rightarrow 6^-$ to judge whether there is or is not an AT line.

Monte Carlo simulations have of course been extensively used in an attempt to understand the nature of spin glasses. Unfortunately in spin glasses, even these state-of-the-art simulations are often plagued by strong finite-size effects. In this paper we study in detail the form which finite-size scaling (FSS) takes as this yields useful information as to whether for $d > 6$ a nonperturbative fixed point or a Gaussian fixed point is controlling the critical behavior.

The paper is structured as follows. In Sec. II we in-

roduce the models studied, as well as the measured observables and scaling functions. In Sec. III we study the universality of the finite-size scaling function for the one-dimensional model with $\sigma < 2/3$ [25, 26], followed by a calculation of the scaling function in Sec. IV. Sections V and VI show results for finite-size scaling at the AT transition, above and below the upper critical dimension, respectively.

II. MODEL, OBSERVABLES AND SCALING FUNCTIONS

In practice, it is difficult to perform finite-size scaling studies on large spin-glass systems when $d > 6$ because the number of sites in a system of linear dimension L increases very rapidly, as L^d , so that the range of L which can be studied is extremely limited. However, it has been realized for some years now that a class of models in one-dimension with long-range interactions falling off with a power of the distance between the spins can serve as a useful proxy for short-range models in high dimension [25–27]. The Hamiltonian of these power-law long-range models is given by

$$\mathcal{H} = - \sum_{ij} J_{ij} S_i S_j - \sum_i h_i S_i, \quad (1)$$

where the sites $i = 1, \dots, N$ lie on a one-dimensional ring to automatically enforce periodic boundary conditions. The sum is over all pairs of sites and the Ising spins $S_i \in \{\pm 1\}$ interact via random couplings J_{ij} . The latter are independent random variables of the form

$$J_{ij} = \epsilon_{ij} / R_{ij}^\sigma, \quad (2)$$

where ϵ_{ij} is a random Gaussian variable with zero mean. It is convenient to take the distance between spin i and spin j , R_{ij} , to be the chord distance between sites i and j , so that $R_{ij} = (N/\pi) \sin(\pi|i-j|/N)$. The variance of ϵ_{ij} is fixed so that $(1/N) \sum_{i,j} J_{ij}^2 = 1$. The fields h_i are drawn from a Gaussian distribution with zero mean and variance H^2 . We shall refer to the case when all the $h_i = 0$ as the zero-field case. Most of our simulational data have been obtained for this one-dimensional proxy for the d dimensional system in previous numerical studies [26, 28–30]. Some of our data have also been obtained for *diluted* versions of the models [31, 32], where an average coordination number $z_b = 6$ is chosen. Details of these diluted models are also to be found in Refs. 27 and 33.

For $\sigma = 0$, this model is the Sherrington-Kirkpatrick (SK) model [6], and for $0 < \sigma < 1/2$ it shares the SK universality class [26, 34]. With our normalization of the bonds, $T_c = 1$ for all $\sigma < 1/2$ when the field $H = 0$. Increasing σ above $1/2$ is thought to be analogous to changing an effective space dimension d of a corresponding short-range model. In the mean-field regime ($d > d_u = 6$) the connection between σ and the equiva-

lent space dimension d is given by [26, 27, 35, 36]

$$d = \frac{2}{2\sigma - 1}. \quad (3)$$

According to Eq. (3) our data for the case $\sigma = 0.55$ therefore corresponds to working in an effective space dimension $d = 20$.

We measure the wave-vector-dependent spin-glass susceptibility defined by

$$\chi_{\text{SG}}(k) = \frac{1}{L} \sum_{i,j} \left[\left(\langle S_i S_j \rangle - \langle S_i \rangle \langle S_j \rangle \right)^2 \right]_{\text{av}} e^{ik(i-j)}. \quad (4)$$

Note that we shall usually simply call $\chi_{\text{SG}}(0)$ the spin-glass susceptibility χ_{SG} . In Eq. (4) $\langle \dots \rangle$ represents a thermal average, whereas $[\dots]_{\text{av}}$ represents an average over the disorder. The finite-size two-point correlation length ξ_L in a system of linear dimension L is given by [33, 37, 38]

$$\xi_L = \frac{1}{2 \sin(k_m/2)} \left[\frac{\chi_{\text{SG}}(0)}{\chi_{\text{SG}}(k_m)} - 1 \right]^{1/(2\sigma-1)}. \quad (5)$$

where $k_m = 2\pi/L$ is the smallest nonzero wave-vector compatible with the periodic boundary conditions. Note that for the one-dimensional model, $L = N$, as $d = 1$, i.e., the linear size of the system is the same as the number of spins N . These two quantities, χ_{SG} and ξ_L are commonly studied in the spin-glass literature, and it is the form of finite-size effects on these quantities which is the subject of this paper.

The scaling form presented in Refs. [34, 39, 40] is different depending on whether behavior is being controlled by a Gaussian fixed point or a nontrivial fixed point. For example, if there is a nontrivial fixed point controlling the critical behavior, the FSS form of the correlation length ξ_L in a system of L^d spins takes the form

$$\xi_L/L = \tilde{\xi} \left[(T - T_c) L^{1/\nu} \right], \quad (6)$$

where the exponent ν is the exponent which describes the growth of the correlation length in the infinite system, where $\xi \sim 1/(T - T_c)^\nu$, and $\tilde{\xi}$ is the finite-size scaling function. However, when the critical behavior is controlled by the Gaussian fixed point, i.e., when one is above the upper critical dimension, $d_u = 6$ [41], ξ_L scales as

$$\xi_L/L^{d/d_u} = \tilde{\xi} \left[(T - T_c) L^{2d/d_u} \right]. \quad (7)$$

Thus, by finding which kind of FSS scaling works best, one can determine the nature of the fixed point which controls the critical behavior.

To apply Eq. (7) to the one-dimensional proxy model, we use Eq. (3) for d on the left of Eq. (7), and on the right side of the equation, we set $L^d = L \equiv N$ for $d = 1$ [34, 40]. Equation (7) therefore becomes for $\sigma = 0.55$

$$\xi_L/L^{1/[3(2\sigma-1)]} \rightarrow \xi_L/L^{10/3} = \tilde{\xi} \left[(T - T_c) L^{1/3} \right]. \quad (8)$$

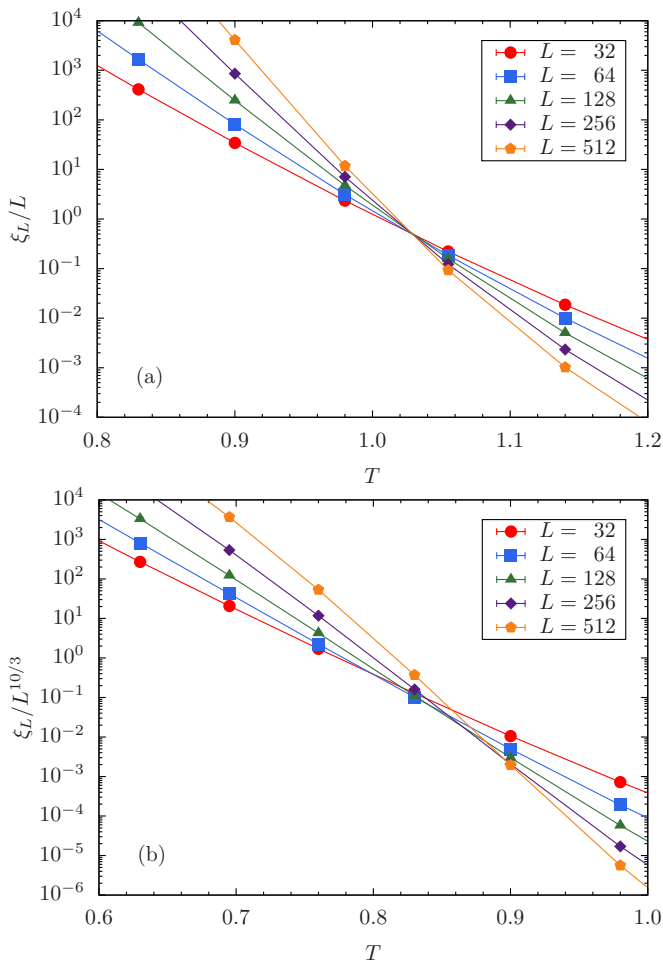


FIG. 1: (Color online) (a) Critical scaling form ξ_L/L versus temperature T for the fully-connected (complete) system with $\sigma = 0.55$ in zero random field H . (b) Mean-field scaling form ξ_L/L versus temperature T for the fully-connected (complete) system with $\sigma = 0.55$ in zero random field H .

Figure 1 shows the two scaling forms based on critical scaling [Eq. (6)] and the mean-field scaling form expected above the upper critical dimension [Eq. (8)]. We had expected that the crossing of the curves for different L values would have been superior for the mean-field scaling form, but this is clearly not the case for the studied system sizes. A similar behavior when searching for the AT line was found by Angelini and Biroli in Ref. 23 and they suggested as a consequence that d_u might not be 6 for spin glasses in a field and that the critical behavior for $d > 6$ might not be controlled by the Gaussian fixed point but by some (as yet) undetermined nonperturbative fixed point.

If one believes in the conventional wisdom that 6 is the upper critical dimension both in zero field and for the AT, then the only possible explanation for the poor mean-field scaling is large corrections to scaling in Fig. 1. On this explanation, if one could obtain data for much larger systems than $L = 512$, then the crossing with mean-

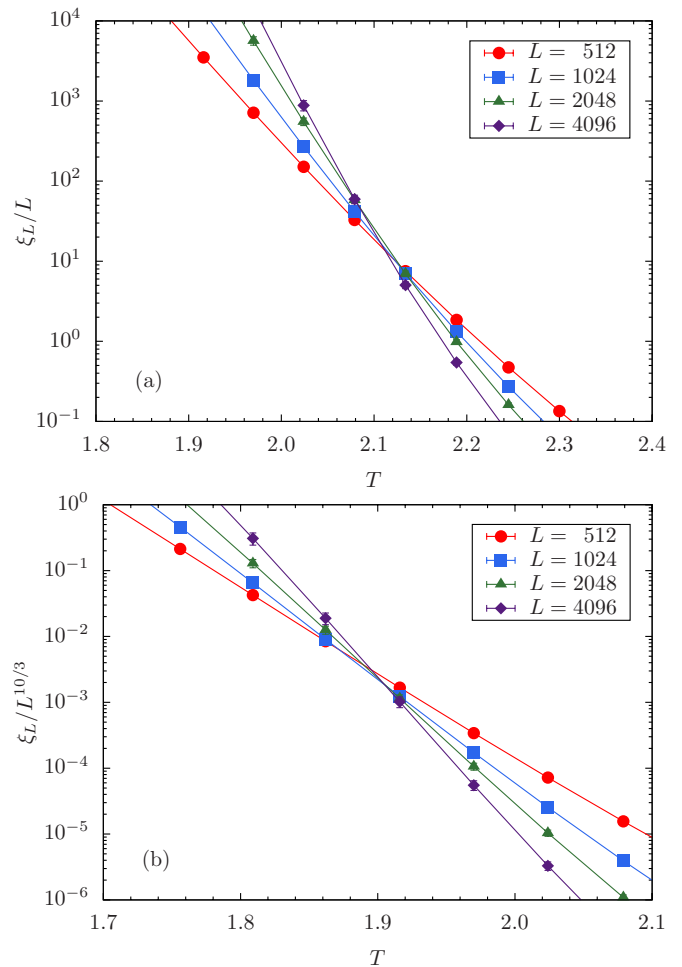


FIG. 2: (Color online) (a) Critical scaling form ξ_L/L versus temperature T for the diluted model with $\sigma = 0.55$ in zero random field H . (b) Mean-field scaling form ξ_L/L versus temperature T for the diluted model with $\sigma = 0.55$ in zero random field H .

field scaling would eventually become better than that for critical scaling. We cannot obtain such data for the fully connected system, but we can for the diluted model and the results for the two kinds of scaling functions are shown in Fig. 2.

There is some evidence that the crossing is indeed improving for the mean-field scaling in these larger systems, but one could not really argue that it is superior to the critical scaling form. Hence, using these simple scaling plots we are unable to provide strong evidence for $d_u = 6$. Instead, we have to resort to an alternate approach to show that mean-field scaling is the correct description of the critical behavior. Our approach is to analytically determine the scaling function $\tilde{\xi}[(T - T_c)L^{1/3}]$ and show that the simulational data fits well to this analytically calculated form. We find that it is possible to do this in zero field and we believe that this is good evidence for the validity of mean-field scaling. In a field, finite-size effects are even larger in numerical work and

on the analytical side we have only been able to extract the asymptotic forms for the scaling functions.

Rather than study the scaling function $\tilde{\xi}$, it is simpler to study the equivalent scaling function for the spin-glass susceptibility $\chi_{\text{SG}}(0)$ obtained from the second moment of the spin-glass order parameter q where

$$q = \frac{1}{N} \sum_i S_i^{(1)} S_i^{(2)}. \quad (9)$$

Here “(1)” and “(2)” refer to two independent copies of the system with the same interactions J_{ij} . We have studied in particular the second moment $q_2 = [\langle q^2 \rangle]_{\text{av}}$ and the quantity

$$\chi_{\text{SG}} = N[\langle q^2 \rangle]_{\text{av}} \quad (10)$$

which is the spin-glass susceptibility in zero field. (Note that in a finite system in zero field $\langle S_i \rangle = 0$). The analogue of the mean-field scaling form in Eq. (8) is [34]

$$\chi_{\text{SG}}/L^{1/3} = \tilde{\chi} \left[(T - T_c)L^{1/3} \right]. \quad (11)$$

The analogue of the critical scaling of Eq. (6) is [34]

$$\chi_{\text{SG}}/L^{2-\eta} = \tilde{\chi} \left[(T - T_c)L^{1/\nu} \right], \quad (12)$$

where $2 - \eta = 2\sigma - 1$. Again, $\tilde{\chi}(x)$ denotes the scaling function, which will also be called $f(x)$. The advantage of studying χ_{SG} rather than ξ_L is that we can study it in the SK universality class where $\sigma < 1/2$, whereas ξ_L is ill-defined for these values of σ . The crossing of $\chi_{\text{SG}}/L^{1/3}$ when plotted against the temperature T for various values of the system size L were studied in Ref. 34 for $\sigma = 0$ and 0.25. For $\sigma = 0.55$ we present in Fig. 3 the corresponding scaling plots.

Notice that in the case of the susceptibility the quality of the crossing is comparable for both the mean-field and critical scaling, whereas for the correlation length the critical scaling form seemed superior, at least for the fully-connected system. However, the temperature at which the curves cross provides an estimate of T_c , and for both χ_{SG} and ξ_L critical scaling is indicating a $T_c > 1$, whereas mean-field scaling indicates a $T_c < 1$. At the level of mean-field theory the transition temperature would be $T_c = 1$, and the fluctuations about the mean field normally reduce the value of of the critical temperature T_c . This clearly is an argument in favor of using the mean-field scaling form. The same observation can be made for the diluted model. For it the mean-field transition temperature is 2.0564 [34], and the estimate of T_c in Fig. 2 for the case of $\sigma = 0.55$ is certainly less than this number using mean-field scaling, but larger than this for the critical scaling form.

Standard finite-size scaling for mean-field scaling takes the form [34]

$$\begin{aligned} \chi_{\text{SG}}(T, L) = & L^{1/3} \left[f(L^{1/3}t) + L^{-\omega} g(L^{1/3}t) + \dots \right] \\ & + d_0 L^{2\sigma-1} h(L^{1/3}t) + c_0 + c_1 t + \dots, \quad (13) \end{aligned}$$

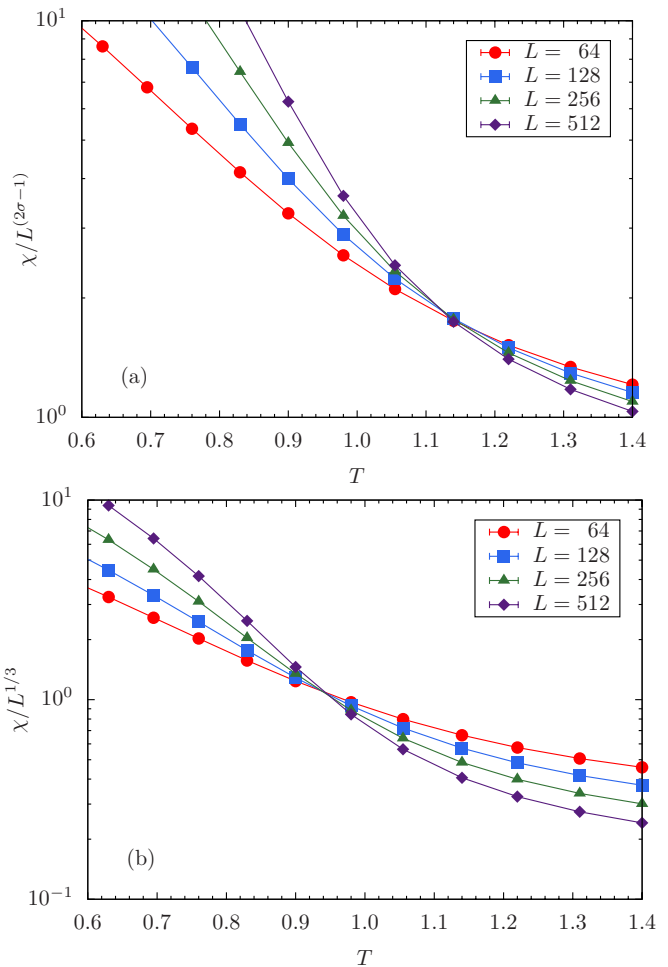


FIG. 3: (Color online) (a) Critical scaling form of the susceptibility $\chi/L^{2\sigma-1}$ vs temperature T for the fully-connected (complete) system with $\sigma = 0.55$ when the random field $H = 0$. (b) Mean-field scaling form $\chi/L^{1/3}$ of the susceptibility $\chi/L^{2\sigma-1}$ vs temperature T for the fully-connected (complete) system with $\sigma = 0.55$ when the random field $H = 0$. Note that $\chi \equiv \chi_{\text{SG}}$.

where $t = T/T_c - 1$, and the correction-to-scaling exponent is $\omega = 2 - 3\sigma$ [25]. In the limit $L \rightarrow \infty$ with $L^{1/3}t$ fixed, this equation reduces to the simpler form

$$\chi_{\text{SG}}/L^{1/3} = f(L^{1/3}t) \quad (14)$$

as then the corrections to scaling become negligible. In what follows, we shall refer to the limit with $x = L^{1/3}t$ fixed as “ $L \rightarrow \infty$ ” as the finite-size scaling limit, and “ $f(x)$ ” as the finite-size scaling function for $\chi_{\text{SG}}/L^{1/3}$.

In Sec. III we outline the Brézin and Zinn-Justin procedure [42] for calculating the universal scaling function $f(x)$ for any space dimension $d > d_u = 6$ (or $\sigma < 2/3$) and show that our simulational data at $\sigma = 0.0, 0.25$, and 0.55 are consistent with being in the same universality class. In Sec. IV we determine $f(x)$ by using the mean-field equations of Thouless, Anderson and Palmer (TAP) [43], as modified by Plefka (TAPP) [44]. We shall

use in Sec. V these same equations to determine the analogue of the scaling function $f(x)$ at the AT transition in nonzero field, however only in the limit of large x . Finally, in Sec. VI we discuss finite-size problems which might make one believe there is an AT line for $d \leq 6$ ($\sigma \geq 2/3$) even though it is absent.

III. UNIVERSALITY OF THE FINITE-SIZE SCALING FUNCTION FOR $\sigma < 2/3$

If the critical behavior is controlled by the Gaussian fixed point, Brézin and Zinn-Justin [42] showed how the finite-size scaling function $f(x)$ can, in principle, be calculated. The procedure basically reduces to calculating the integral

$$\overline{Z^n} = \int dQ_{\alpha\beta} \exp[-F[\{Q_{\alpha\beta}\}]/kT], \quad (15)$$

where

$$F[\{Q_{\alpha\beta}\}]/kT = \int d^d x \left[\frac{1}{2} r \sum_{\alpha < \beta} Q_{\alpha\beta}^2 + \frac{w}{6} \sum_{\alpha < \beta < \gamma} Q_{\alpha\beta} Q_{\beta\gamma} Q_{\gamma\alpha} + \mathcal{O}(Q^4) \right]. \quad (16)$$

The coefficient r is essentially a measure of the distance from T_c , i.e., it is related to the reduced temperature t . The Q^4 -terms are irrelevant when calculating the scaling function, as are the usual density gradient terms $(\nabla Q_{\alpha\beta})^2$ seen in such free-energy functionals [41], although they would have been needed if we had tried to calculate the scaling function associated with ξ_L . $Q_{\alpha\beta}$ is related to the spin-glass order parameter, and α takes the values $1, 2, \dots, n$, with $n \rightarrow 0$. This integral should be adequate for calculating the crossover scaling function $f(x)$ in the mean-field scaling regime, i.e., for all $\sigma < 2/3$. The form of the function is universal, and the differences between fully-connected spins or the diluted version of the model, or the value of σ , just feed into the value of T_c , the overall amplitude of $\chi_{SG}/L^{1/3}$ and a multiplicative factor associated with t . For $\sigma > 2/3$, when the behavior is not controlled by the Gaussian fixed point but instead by the critical fixed point [41], the calculation of the scaling function is more complicated. Its argument changes to $L^{1/\nu}t$ and the scaling function is different from the universal form expected to apply for all $\sigma < 2/3$.

In Fig. 4 we plot results for $\chi_{SG}/N^{1/3}$ versus the scaling variable $x = (T/T_c - 1)N^{1/3}$ for $\sigma = 0.0, 0.25$, and 0.55 for both the fully-connected (complete) model and for the diluted model. The points include data for all the system sizes N simulated (see caption). In the range $1 > x > -3$ there is a fairly satisfactory collapse of the data onto a single curve for the differing values of σ and for both the fully-connected and dilute models. None of

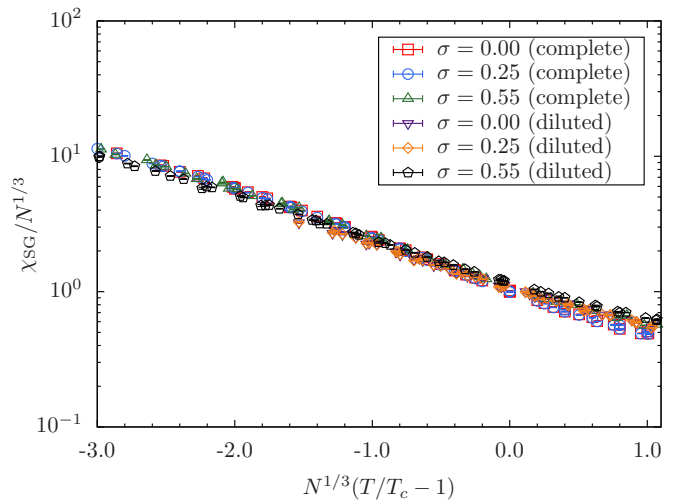


FIG. 4: (Color online) Reduced spin-glass susceptibility $\chi_{SG}/N^{1/3}$ versus $x = N^{1/3}(T/T_c - 1)$, (recall, $N \equiv L$), i.e., the finite-size scaling function $f(x)$ in zero field for all system sizes N studied. For the SK model ($\sigma = 0$) we simulated $N = 1024, \dots, 4096$. For the diluted model and $\sigma = 0$ we studied $N = 2048, \dots, 16384$. For $\sigma = 0.25$ we studied $N = 512, \dots, 4096$ for the complete (fully-connected) model and $N = 2048, \dots, 16384$ for the diluted model. Data taken from Ref. 34. For $\sigma = 0.55$ we studied $N = 32, \dots, 512$ for the complete (fully-connected) model and $N = 128, \dots, 2048$ for the diluted model. Data taken from Refs. 26 and 27. For $\sigma = 0.55$ for the complete (fully-connected) case we have taken $T_c \approx 0.94$, while for the diluted case we use $T_c \approx 1.98$. Note the vertical logarithmic scale.

the data have been linearly scaled on either the horizontal or vertical axes of the figure, which would have been permissible while staying in the same universality class. The data for $x > 1$ are strongly affected by finite-size effects, some of which can be seen in Fig. 5, which is why in Fig. 4 we have limited the horizontal range to $x < 1$.

Overall the data are consistent with a universal scaling function $f(x)$ for $\sigma < 2/3$. If the behavior were controlled by a nonperturbative fixed point rather than by the Gaussian fixed point, then such universality of $f(x)$ would have to be understood. Furthermore, as we shall see in Sec. IV below, it is possible to calculate the function $f(x)$ explicitly. Our results in Fig. 5 turn out to be in satisfactory agreement with our approximation.

It is possible to determine the behavior of $f(x)$ as $x \rightarrow \pm\infty$ by simple arguments: When $x \rightarrow -\infty$, $\chi_{SG} \rightarrow Nq^2$, and as $q \rightarrow -t$ in the scaling limit where $t \rightarrow 0$, that means that $f(x) \rightarrow x^2$. The data in Fig. 5 are approaching this estimate at large negative x . For $x \rightarrow \infty$, $\chi_{SG} \rightarrow 1/(1 - \beta^2)$ [see Eq. (25)] for the SK model and also from the TAPP equations, which implies that $f(x) \rightarrow 1/(2x)$ as $\beta = 1/(1 + t)$. Again, the data shown in Fig. 5 seem to be approaching this limit, but the finite-size effects are large for positive x . This is not due to any inaccuracies in the TAPP equations, but just points to the fact that in order to use the simplification

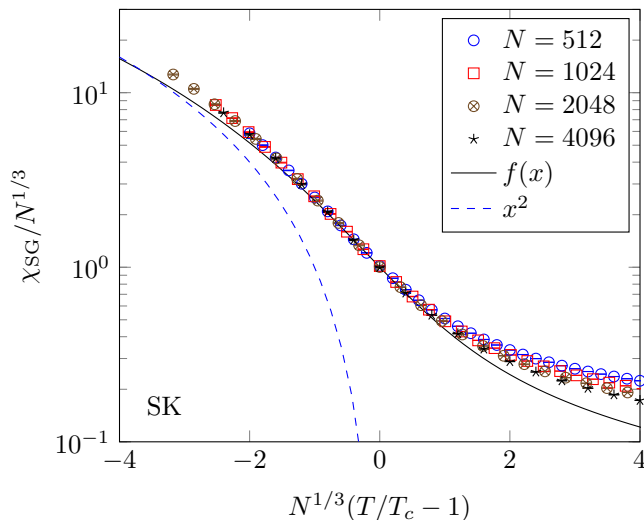


FIG. 5: (Color online) Reduced spin-glass susceptibility $\chi_{\text{SG}}/N^{1/3}$ versus $x = N^{1/3}(T/T_c - 1)$, i.e., the finite-size scaling function $f(x)$ in zero field for the SK model ($\sigma = 0$). The data are taken from Ref. 34. For this model $T_c = 1$ [6]. The data for $x > 1$ are strongly affected by finite-size effects. The solid curve shows our approximation based on Eq. (29) for the scaling function $f(x)$ based on solving the TAPP equations. It gives, at large positive x , $f(x) \rightarrow 1/(2x)$, while at large negative x , $f(x) \rightarrow x^2$. The blue dashed curve is the asymptotic limit $f(x) \rightarrow x^2$ for negative x values.

$\chi_{\text{SG}} = 1/(2t)$ [which leads to $f(x) \rightarrow 1/(2x)$] one needs to work with rather small values of t . However, at fixed large x , this requires working with very large values of N , which are currently not accessible numerically.

IV. CALCULATION OF THE SCALING FUNCTION $f(x)$

In this section we outline how one can calculate the finite-size scaling function $f(x)$. One approach would be to simply do the integrals in Eq. (15). Unfortunately, that is very difficult because of the replica labels and the need to continue $n \rightarrow 0$. However, an approach equivalent to this was used by three of us in Ref. 45 and it results in studying the finite-size scaling function for the spherical SK spin-glass model, which according to the arguments in aforementioned reference should have an identical scaling function $f(x)$. However, this approach is hard to extend to the behavior in a field, so instead we present an approach which does permit, in principle, an extension to finite fields.

Assuming that the scaling function $f(x)$ applies for all $\sigma < 2/3$, if we can calculate it for the SK model with $\sigma = 0$ and that agrees with data for (say) $\sigma = 0.55$ —as is the case in Fig. 4—then the assumption would seem to be correct. To calculate $f(x)$ for the SK model we use the TAP equations [43] as modified by Plefka [44] and refer to them as the TAPP equations. Plefka argued

that in the presence of an external field h_i at each site i , the magnetization m_i is given by

$$m_i = \tanh \beta \left[h_i + \sum_j J_{ij} m_j - m_i \chi_\ell \right], \quad (17)$$

where the local susceptibility is given by

$$\chi_\ell = N^{-1} \sum_i \chi_{ii} = N^{-1} \sum_i \partial m_i / \partial h_i. \quad (18)$$

Plefka assumed that $\partial \chi_\ell / \partial m_i$ is of order $\mathcal{O}(N^{-1})$ and thus negligible when the inverse susceptibility matrix is calculated from Eq. (17)

$$\chi_{ij}^{-1} = \delta_{ij} [\beta^{-1} (1 - m_i^2)^{-1} + \chi_\ell] - J_{ij}. \quad (19)$$

Equations (17) and (19), with $\sum_j \chi_{ij} \chi_{jk}^{-1} = \delta_{ik}$ form a closed set of equations for the m_i and χ_ℓ . They are not exact, unfortunately, as the terms of $\mathcal{O}(N^{-1})$ can, for certain quantities, combine to make $\mathcal{O}(1)$ contributions [46]. We believe that such possibilities are unimportant in our calculation of $f(x)$. Our argument for this is that the use of these equations gives in our finite-size scaling limit the same results as can be obtained by the spherical model SK spin glass mapping [45], which we think is exact in zero field. For zero fields, in our scaling regime, $m_i \rightarrow 0$, and Eq. (19) simplifies to

$$\chi_{ij}^{-1} = \delta_{ij} [\beta^{-1} + \chi_\ell] - J_{ij}. \quad (20)$$

The self-consistency equation for χ_ℓ is then conveniently written in terms of $z = \beta^{-1} + \chi_\ell$ as

$$z - \beta^{-1} = N^{-1} \sum_i \frac{1}{z - \lambda_i}, \quad (21)$$

where λ_i are the eigenvalues of the matrix J_{ij} . The physical solution is the solution which has the largest real value of z .

In the large- N limit, the N real eigenvalues λ_i are described by the semi-circle distribution with support between -2 and 2 . Then Eq. (21) reduces to

$$z - \beta^{-1} = 1 + \frac{(z - 2) - \sqrt{(z - 2)(z + 2)}}{2}, \quad (22)$$

which gives $z = \beta + \beta^{-1}$. We want to calculate

$$\begin{aligned} \chi_{\text{SG}} &\equiv \frac{1}{\beta^2} N^{-1} \sum_{i,j} \chi_{ij}^2 \\ &= \frac{1}{\beta^2} N^{-1} \sum_i \frac{1}{(z - \lambda_i)^2}. \end{aligned} \quad (23)$$

In the large- N limit, the sum can be done and gives

$$\frac{1}{2\beta^2} \frac{z}{\sqrt{z^2 - 4} - 1}, \quad (24)$$

which reduces to

$$\chi_{\text{SG}} \rightarrow \frac{1}{1 - \beta^2}, \quad (25)$$

on substituting $z = \beta + \beta^{-1}$. It is this result which we use to determine the limit of $f(x)$ as $x \rightarrow \infty$ (see Fig. 6).

In principle, for finite N values, one could solve for z numerically using Eq. (21). However, this is difficult for large N . Instead, we give an approximate solution which seems in practice to be quite accurate. As $x \rightarrow -\infty$, $z \rightarrow \lambda_{\text{max}}$ and throughout the scaling region differs from λ_{max} by terms of $\mathcal{O}(1/N^{2/3})$. The largest eigenvalue itself has the form $\lambda_{\text{max}} = 2 + \mathcal{O}(1/N^{2/3})$. Let us introduce the variable $u = (z - \lambda_{\text{max}})N^{2/3} > 0$ and the notation $\Delta = (\lambda_{\text{max}} - \lambda_1)N^{2/3}$, where λ_1 is the next largest eigenvalue. Then we separate off the first two terms in the sum in Eq. (21) and approximate the rest by Eq. (22) after replacing $(z - 2)$ by $(z - \lambda_{\text{max}})$ [45]. The left-hand-side of Eq. (21) becomes

$$z - \beta^{-1} \rightarrow 1 - x/N^{1/3} + \mathcal{O}(1/N^{2/3}). \quad (26)$$

The right-hand side becomes

$$\frac{1}{N^{1/3}u} + \frac{1}{N^{1/3}(u + \Delta)} + 1 - \sqrt{u/N^{2/3}} + \mathcal{O}(1/N^{2/3}). \quad (27)$$

Thus, correct to $\mathcal{O}(1/N^{2/3})$, we have as our basic approximation for u ,

$$-x = \frac{1}{u} + \frac{1}{u + \Delta} - \sqrt{u}. \quad (28)$$

Within the same approximation, the sample with gap Δ gives for $f(x)$

$$f(x) = \frac{1}{u^2} + \frac{1}{(u + \Delta)^2} + \frac{1}{2\sqrt{u}}. \quad (29)$$

To calculate the bond-averaged value of $f(x)$ we must average over the spacing Δ which we do with the Wigner surmise distribution for it [47].

Before comparing with the numerical data we need to introduce the pseudo-critical temperature $T_c(N)$ [48, 49]. If one studies the function $-f'(x)/f(x)$, it has a peak at T_c . However, in a system of finite size N , this peak is shifted to $T_c(N)$, where in the mean-field regime,

$$T_c(N) = T_c - \frac{a}{N^{1/3}}. \quad (30)$$

For the SK model $T_c = 1$ and typical values for a are ~ 0.2 , but this depends on the function being studied [48]. When trying to construct the universal scaling function $f(x)$ for different models it is natural to shift the horizontal axis so that the peaks for the different models coincide at $x = 0$, which can be done by redefining x so that $x = [T/T_c(N) - 1]N^{1/3}$. This definition of x differs from the old definition by $a + \mathcal{O}(1/N^{1/3})$. Thus, when comparing to our numerical data, one can shift the

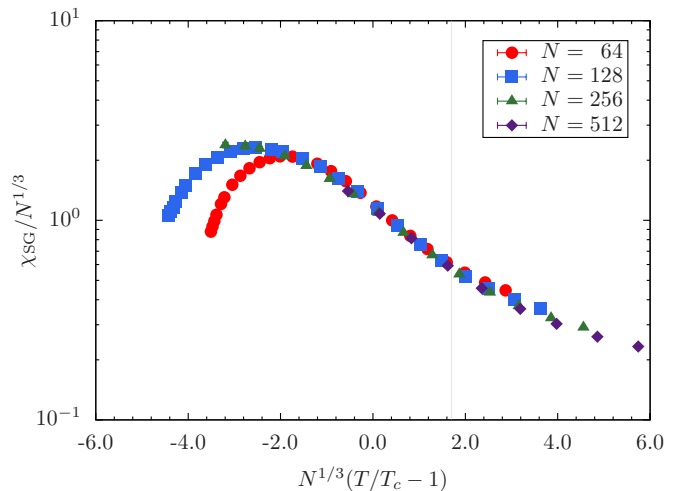


FIG. 6: (Color online) Reduced spin-glass susceptibility $\chi_{\text{SG}}/N^{1/3}$ versus $x = N^{1/3}[T/T_c(H) - 1]$, that is the finite-size scaling function $f_H(x)$ in a random field of standard deviation 0.10 when $\sigma = 0.55$. For this model $T_c(H = 0.1) \approx 0.815$.

curves by an amount a to improve the fit, and this is what we did in Fig. 5. With this shift, the overall agreement is quite satisfactory, considering the simplicity of the approximation. We suspect that it might be possible to calculate $f(x)$ exactly, but that remains a challenge for the future.

V. FINITE-SIZE SCALING AT THE ALMEIDA-THOULESS TRANSITION

In this section we shall discuss finite-size scaling at the AT transition [21]. The upper critical dimension of the AT line is expected to be the same as in zero field, that is, $d_u = 6$ [50]. For the long-range model, that translates to $\sigma = 2/3$. Note that in a field $\langle S_i \rangle$ is non-zero, and we have to study the cumulant second moment, i.e.,

$$\chi_{\text{SG}} = \frac{1}{N} \sum_{i,j} [\langle S_i S_j \rangle - \langle S_i \rangle \langle S_j \rangle]_{\text{av}}^2. \quad (31)$$

In a field we only have numerical data for the one-dimensional long-range model with $\sigma = 0.55$. In Fig. 6 we show the mean-field scaling form $\chi_{\text{SG}}/N^{1/3} = f_H(x)$ against $x = N^{1/3}[T/T_c(H) - 1]$. The finite-size effects are strongly visible on the low-temperature side of the transition.

We now turn to understanding the form of the finite-size scaling function $f_H(x)$ near the AT transition. At the formal level, the analogue of Eq. (16) for the AT transition involves just the fields in the replicon sector $\tilde{Q}_{\alpha\beta}$, which are such that $\sum_{\beta} \tilde{Q}_{\alpha\beta} = 0$ [50]. The replicated partition function is

$$\overline{Z^n} = \int d\tilde{Q}_{\alpha\beta} \exp \left[-F[\{\tilde{Q}_{\alpha\beta}\}]/kT \right], \quad (32)$$

where the effective functional is

$$F[\{\tilde{Q}_{\alpha\beta}\}]/kT = \int d^d x \left[\frac{1}{4} \tilde{r} \sum \tilde{Q}_{\alpha\beta}^2 + \frac{w_1}{6} \sum \tilde{Q}_{\alpha\beta} \tilde{Q}_{\beta\gamma} \tilde{Q}_{\gamma\alpha} + \frac{w_2}{6} \sum \tilde{Q}_{\alpha\beta}^3 \right]. \quad (33)$$

Here the convention has been adopted that the sums over replica indices are unrestricted. Note that $\tilde{Q}_{\alpha\alpha} = 0$. At the AT line, $\tilde{r} = 0$ in the mean-field approximation and the two couplings w_1 and w_2 both depend on the field H . We would expect as a consequence the finite-size scaling function $f_H(x)$ to depend on both x and the strength of the field H . It is because the effective field theory is a cubic field theory that the upper critical dimension $d_u = 6$ for the AT line [50]. Unfortunately, the integrals in Eq. (33) needed to calculate $f_H(x)$ are even more difficult to do than those of the zero-field case and other methods have to be used to understand the finite-size scaling function $f_H(x)$.

We have tried solving the TAPP equations for the SK limit in the presence of a field numerically. We obtained the solution for a given bond and field realization at high temperatures, and followed the solution down to lower temperatures, for N values up to 400. At temperatures well above $T_c(H)$, we obtained values for χ_{SG} consistent with those in Fig. 6. At large positive values of x one is effectively in the regime where one can use the locator expansion [51] on the TAPP equations. The result [44] is that Eq. (25) is generalized to

$$\chi_{\text{SG}} \rightarrow \frac{\chi_{\text{SG}}^0}{1 - \beta^2 \chi_{\text{SG}}^0}, \quad (34)$$

where [52]

$$\chi_{\text{SG}}^0 = \frac{1}{N} \sum_i (1 - m_i^2)^2. \quad (35)$$

We stress that this result holds just for the large- N limit and $T > T_c(H)$. For the SK model in a random field H , χ_{SG}^0 can be determined explicitly. At the AT transition $T_c(H)$, $\chi_{\text{SG}}^0 = T_c(H)^2$, and so for T close to $T_c(H)$,

$$\chi_{\text{SG}} \rightarrow \frac{T_c(H)^2}{[1 - \beta T_c(H)][1 + \beta T_c(H)]} \rightarrow \frac{1}{2t} T_c(H)^2, \quad (36)$$

where $t = [T/T_c(H) - 1]$. For $H = 0.1$, $T_c(0.1) = 0.819428$ for the SK model, so $\chi_{\text{SG}} \rightarrow 0.33573/t$. Unfortunately, the data in Fig. 6 have not been obtained at large enough values of N (here the largest N value is 512) or small enough values of t , to see this behavior clearly. However, the calculated values of χ_{SG} are consistent with the result presented in Eq. (34).

As the temperature is reduced to well below $T_c(H)$, the solution of the TAPP equations in the large- N limit is expected to reduce to $\chi_{\text{SG}} \rightarrow 1/|t|$ [44]. For the N values for which we could obtain solutions, i.e., $N < 400$, this behavior was not visible. In fact, most samples

showed a peak in χ_{SG} well above $T_c(H)$, followed by a fall at lower temperatures. We suspect that the fall at low temperatures visible in Fig. 6 might be connected with the fall seen in the TAPP equations. The decrease in $\chi_{\text{SG}}/N^{1/3}$ at large negative x values seen in Fig. 6 is clearly a finite-size effect.

We suspect that in the absence of finite-size effects $f_H(x)$ would actually continue to grow $\propto x^2$ at large negative x , due to replica symmetry breaking effects [53], and not follow the expectations based on the solution of the TAPP equations, which would be that $f(x) \rightarrow 1/|x|$. In Ref. 53 it was shown that for the SK model, where the Parisi RSB broken order parameter is $q(x)$,

$$\chi_{\text{SG}} = \frac{N}{3} \left\{ \int_0^1 q^2(x) dx - \left[\int_0^1 q(x) dx \right]^2 \right\}. \quad (37)$$

At large negative x one would therefore expect that because of these replica symmetry breaking effects that $f_H(x) \rightarrow Bx^2$ so that χ_{SG} is proportional to N . Using the results in Refs. 53 and 54 for $q(x)$ in a field, one can calculate the coefficient B and it is of order q_{EA} on the AT line, which is small (≈ 0.2) when $H = 0.1$. However, the data in Fig. 6 at negative x values are not extensive enough to provide a clear verification of these predictions.

VI. NUMERICAL SEARCHES FOR THE ALMEIDA-THOULESS LINE WHEN $d \leq 6$ ($\sigma \geq 2/3$)

In Sec. I we stated that there is likely no AT line when $d \leq 6$. As a consequence, we were surprised when Castellana and Parisi [24] recently claimed that in the Dyson hierarchical model numerical evidence suggested the existence of an AT line at $\sigma = 0.68 > 2/3$ which corresponds to an effective space dimension $d < 6$. At the transition they reported values for the critical exponents which were not close to their mean-field values, which lead them to suggest that the behavior was being controlled by a non-perturbative fixed point.

In this section we discuss a problem which arises when trying to determine the existence of the AT line in dimensions where there might be no AT line. It is again a finite-size problem. If there is no AT line and the droplet picture applies, then the correlation length ξ_D in the system is the Imry-Ma length [55], determined by equating the free energy cost of flipping a region of size ξ_D , $kT_c(\xi_D/\xi)^\theta$ to the energy which might be gained from the random applied field, which is $\sqrt{q}H\xi_D^{d/2}$ (see for example, Ref. 56). Here ξ denotes the zero-field correlation length $\sim 1/|t|^\nu$. In our one-dimensional model, $\theta = 1 - \sigma$ [57]. Then

$$\frac{\xi_D}{\xi} \sim \left[\frac{H_{\text{AT}}}{H} \right]^{2/(2\sigma-1)}, \quad (38)$$

where

$$H_{\text{AT}} \equiv kT_c |t|^{(\gamma+\beta)/2}, \quad (39)$$

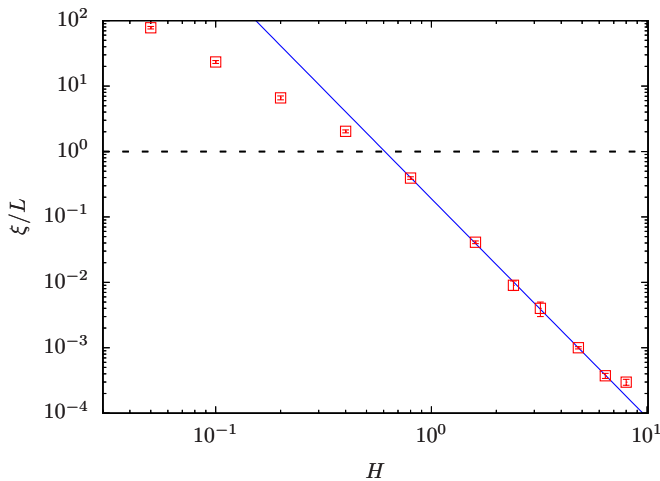


FIG. 7: (Color online) Correlation length ξ_L/L over a large range of field values for $L = 1024$, $T = 0.48$, and $\sigma = 0.75$. The horizontal dashed line is a guide to the eye marking the point where $\xi_L = L$. A change in behavior for $\xi < L$ is apparent. The solid (blue) line marks the regime where the Imry-Ma argument [55] is valid.

which is the scaling expectation for the form of the AT line [56], should it exist. At the borderline value of $\sigma = 2/3$, ξ_D grows rapidly for small fields $\propto 1/H^6$. In order to see droplet behavior one requires system sizes $L > \xi_D$. Otherwise, one might be tempted to think there is an AT line. For $\sigma = 0.75$ we plot ξ_L/L as a function of the field H in Fig. 7. Here, ξ_D grows at small $H \propto 1/H^4$. Figure 7 shows that the droplet model prediction that $\xi_L \sim \xi_D$ fails when $\xi_L > L$, as then finite-size effects are clearly making ξ_L deviate away from ξ_D . The basic message is that to see droplet model behavior one needs to study system sizes $L > \xi_D$. When studying fields where $\xi_D > L$, one can be misled into thinking there is evidence for an AT line, as discussed at great length in Ref. 33. We suspect this is why the authors of Ref. 24 thought there was an AT line at $\sigma = 0.68$. In fact, the growth of ξ_D as $1/H^6$ when $\sigma \rightarrow 2/3^+$ will always make it very difficult to obtain data for the regime where $L > \xi_D$.

VII. CONCLUSIONS

We have studied finite-size effects on critical scaling in Ising spin glasses both in zero field and finite field in the regime where mean-field scaling is expected. We believe that the conventional wisdom that both types of transition have 6 as the upper critical dimension is supported by the numerical data gathered from previous studies, even though strong finite-size effects are present. For the zero-field case, we have found a simple approximation for the crossover function for the spin-glass susceptibility. The finite-field case is far more difficult, but we have been able to determine the asymptotic form of the crossover function by allowing for the non-self-averaging

features of the Parisi order parameter $q(x)$ which occur below the AT transition.

We should point out that there is a lack of self-averaging generally throughout the critical scaling regime. Thus, in zero field, we have studied in the SK limit the distribution function of χ_{SG} at $T = T_c$ which arises from different realizations of the bonds J_{ij} that has a well-defined distribution. The zero-field problem seems sufficiently simple such that one day the scaling function $f(x)$ might be determined analytically; as a by-product one might then obtain the corresponding distribution functions.

We have argued previously that evidence for an AT line when $d < 6$ might be just a consequence of not allowing for the effects of finite-size effects. In order to see the droplet picture emerging clearly, one needs the linear system size L to be larger than the Imry-Ma length ξ_D . However, this length scale can be very long at the fields commonly used in most numerical studies. This means that when $L \leq \xi_D$ one can easily be misled into believing that there is a transition in a field. For example, from the data presented in Fig. 7 for the one-dimensional model with $\sigma = 0.75$, one needs system sizes L larger than 1024 sites, as well as fields stronger than $H_R \approx 0.7$ to see the droplet behavior. Our hope is that future studies first verify the needed system sizes $L > \xi_D$ before claiming the existence of a spin-glass state in a field.

Acknowledgments

We thank Peter Young for participating in the initial stages of this work and providing extremely useful feedback on this project. Furthermore, we thank Satya Majumdar and Yan Fyodorov for discussions on the possibility of calculating the scaling function $f(x)$ exactly, as well as Leo Alcorn for providing help with GraphClick [58] (used to digitize the data in Fig. 7). J. Y. was supported by Basic Science Research Program through the National Research Foundation of Korea (NRF) funded by the Ministry of Education (2014R1A1A2053362). M. W. was supported through the National Science Foundation (Grant No. DMR-1207036). H. G. K. acknowledges support from the National Science Foundation (Grant No. DMR-1151387) and would like to thank Hitachino Nest for inspiration. H. G. K.'s research is based upon work supported in part by the Office of the Director of National Intelligence (ODNI), Intelligence Advanced Research Projects Activity (IARPA), via MIT Lincoln Laboratory Air Force Contract No. FA8721-05-C-0002. The views and conclusions contained herein are those of the authors and should not be interpreted as necessarily representing the official policies or endorsements, either expressed or implied, of ODNI, IARPA, or the U.S. Government. The U.S. Government is authorized to reproduce and distribute reprints for Governmental purpose notwithstanding any copyright annotation thereon. We thank ETH Zurich for access to their Brutus clus-

ter, the Texas Advanced Computing Center (TACC) at The University of Texas at Austin for providing HPC re-

sources (Stampede cluster), and Texas A&M University for access to their Ada, Curie, Eos and Lonestar clusters.

-
- [1] G. Parisi, *Infinite number of order parameters for spin-glasses*, Phys. Rev. Lett. **43**, 1754 (1979).
- [2] G. Parisi, *The order parameter for spin glasses: a function on the interval 0–1*, J. Phys. A **13**, 1101 (1980).
- [3] G. Parisi, *A sequence of approximated solutions to the S-K model for spin glasses*, J. Phys. A **13**, L115 (1980).
- [4] G. Parisi, *Order parameter for spin-glasses*, Phys. Rev. Lett. **50**, 1946 (1983).
- [5] M. Mézard, G. Parisi, N. Sourlas, G. Toulouse, and M. Virasoro, *Nature of the Spin-Glass Phase*, Phys. Rev. Lett. **52**, 1156 (1984).
- [6] D. Sherrington and S. Kirkpatrick, *Solvable model of a spin glass*, Phys. Rev. Lett. **35**, 1792 (1975).
- [7] D. S. Fisher and D. A. Huse, *Ordered phase of short-range Ising spin-glasses*, Phys. Rev. Lett. **56**, 1601 (1986).
- [8] D. S. Fisher and D. A. Huse, *Equilibrium behavior of the spin-glass ordered phase*, Phys. Rev. B **38**, 386 (1988).
- [9] D. S. Fisher and D. A. Huse, *Nonequilibrium dynamics of spin glasses*, Phys. Rev. B **38**, 373 (1988).
- [10] A. J. Bray and M. A. Moore, *Scaling theory of the ordered phase of spin glasses*, in *Heidelberg Colloquium on Glassy Dynamics and Optimization*, edited by L. Van Hemmen and I. Morgenstern (Springer, New York, 1986), p. 121.
- [11] W. L. McMillan, *Domain-wall renormalization-group study of the two-dimensional random Ising model*, Phys. Rev. B **29**, 4026 (1984).
- [12] C. M. Newman and D. L. Stein, *Multiple states and thermodynamic limits in short-ranged Ising spin-glass models*, Phys. Rev. B **46**, 973 (1992).
- [13] C. M. Newman and D. L. Stein, *Non-mean-field behavior of realistic spin glasses*, Phys. Rev. Lett. **76**, 515 (1996).
- [14] C. M. Newman and D. L. Stein, *Simplicity of state and overlap structure in finite-volume realistic spin glasses*, Phys. Rev. E **57**, 1356 (1998).
- [15] C. M. Newman and D. L. Stein, *TOPICAL REVIEW: Ordering and broken symmetry in short-ranged spin glasses*, J. Phys.: Condensed Matter **15**, 1319 (2003).
- [16] C. M. Newman and D. L. Stein, *Short-range spin glasses: Results and speculations*, in *Lecture Notes in Mathematics 1900* (Springer-Verlag, Berlin, 2007), p. 159, (condmat/0503345).
- [17] D. L. Stein and C. M. Newman, *Spin Glasses and Complexity*, Primers in Complex Systems (Princeton University Press, 2013).
- [18] M. A. Moore and A. J. Bray, *Disappearance of the de Almeida-Thouless line in six dimensions*, Phys. Rev. B **83**, 224408 (2011).
- [19] Criticisms of this argument [59] were further discussed in a very recent paper by two of us [56].
- [20] T. S. Jackson and N. Read, *Theory of minimum spanning trees. I. Mean-field theory and strongly disordered spin-glass model*, Phys. Rev. E **81**, 021130 (2010).
- [21] J. R. L. de Almeida and D. J. Thouless, *Stability of the Sherrington-Kirkpatrick solution of a spin glass model*, J. Phys. A **11**, 983 (1978).
- [22] M. Castellana and C. Barbieri, *Hierarchical spin glasses in a magnetic field: A renormalization-group study*, Phys. Rev. B **91**, 024202 (2015).
- [23] M. C. Angelini and G. Biroli, *Spin Glass in a Field: A New Zero-Temperature Fixed Point in Finite Dimensions*, Phys. Rev. Lett. **114**, 095701 (2015).
- [24] M. Castellana and G. Parisi, *Non-perturbative effects in spin glasses*, Sci. Rep. **5**, 8697 (2015).
- [25] G. Kotliar, P. W. Anderson, and D. L. Stein, *One-dimensional spin-glass model with long-range random interactions*, Phys. Rev. B **27**, 602 (1983).
- [26] H. G. Katzgraber and A. P. Young, *Monte Carlo studies of the one-dimensional Ising spin glass with power-law interactions*, Phys. Rev. B **67**, 134410 (2003).
- [27] H. G. Katzgraber, D. Larson, and A. P. Young, *Study of the de Almeida-Thouless line using power-law diluted one-dimensional Ising spin glasses*, Phys. Rev. Lett. **102**, 177205 (2009).
- [28] H. G. Katzgraber and A. P. Young, *Geometry of large-scale low-energy excitations in the one-dimensional Ising spin glass with power-law interactions*, Phys. Rev. B **68**, 224408 (2003).
- [29] H. G. Katzgraber and A. P. Young, *Probing the Almeida-Thouless line away from the mean-field model*, Phys. Rev. B **72**, 184416 (2005).
- [30] H. G. Katzgraber, *Spin glasses and algorithm benchmarks: A one-dimensional view*, J. Phys.: Conf. Ser. **95**, 012004 (2008).
- [31] L. Leuzzi, G. Parisi, F. Ricci-Tersenghi, and J. J. Ruiz-Lorenzo, *Diluted One-Dimensional Spin Glasses with Power Law Decaying Interactions*, Phys. Rev. Lett. **101**, 107203 (2008).
- [32] L. Leuzzi, G. Parisi, F. Ricci-Tersenghi, and J. J. Ruiz-Lorenzo, *Bond diluted Levy spin-glass model and a new finite size scaling method to determine a phase transition*, Philos. Mag. **91**, 1917 (2011).
- [33] D. Larson, H. G. Katzgraber, M. A. Moore, and A. P. Young, *Spin glasses in a field: Three and four dimensions as seen from one space dimension*, Phys. Rev. B **87**, 024414 (2013).
- [34] M. Wittmann and A. P. Young, *Spin glasses in the nonextensive regime*, Phys. Rev. E **85**, 041104 (2012).
- [35] L. Leuzzi, G. Parisi, F. Ricci-Tersenghi, and J. J. Ruiz-Lorenzo, *Ising Spin-Glass Transition in a Magnetic Field Outside the Limit of Validity of Mean-Field Theory*, Phys. Rev. Lett. **103**, 267201 (2009).
- [36] R. A. Baños, L. A. Fernandez, V. Martin-Mayor, and A. P. Young, *Correspondence between long-range and short-range spin glasses*, Phys. Rev. B **86**, 134416 (2012).
- [37] H. G. Ballesteros, A. Cruz, L. A. Fernandez, V. Martin-Mayor, J. Pech, J. J. Ruiz-Lorenzo, A. Tarancon, P. Tellez, C. L. Ullod, and C. Ungil, *Critical behavior of the three-dimensional Ising spin glass*, Phys. Rev. B **62**, 14237 (2000).
- [38] H. G. Katzgraber, M. Körner, and A. P. Young, *Universality in three-dimensional Ising spin glasses: A Monte Carlo study*, Phys. Rev. B **73**, 224432 (2006).
- [39] J. L. Jones and A. P. Young, *Finite size scaling of the correlation length above the upper critical dimension*, Phys.

- Rev. B **71**, 174438 (2005).
- [40] M. Wittmann and A. P. Young, *Finite-size scaling above the upper critical dimension*, Phys. Rev. E **90**, 062137 (2014).
- [41] A. B. Harris, T. C. Lubensky, and J.-H. Chen, *Critical Properties of Spin-Glasses*, Phys. Rev. Lett. **36**, 415 (1976).
- [42] E. Brézin and J. Zinn-Justin, *Finite size effects in phase transitions*, Nucl. Phys. B **257**, 867 (1985).
- [43] D. J. Thouless, P. W. Anderson, and R. G. Palmer, *Solution of ‘Solvable model of a spin glass’*, Phil. Mag. **35**, 593 (1977).
- [44] T. Plefka, *Modified TAP equations for the SK spin glass*, Europhys. Lett. **58**, 892 (2002).
- [45] J. Yeo, M. A. Moore, and T. Aspelmeier, *Nature of perturbation theory in spin glasses*, J. Phys. A **38**, 4027 (2005).
- [46] T. Aspelmeier, A. J. Bray, and M. A. Moore, *Why Temperature Chaos in Spin Glasses Is Hard to Observe*, Phys. Rev. Lett. **89**, 197202 (2002).
- [47] G. J. Rodgers and M. A. Moore, *Distribution of barrier heights in infinite-range spin glass models*, J. Phys. A **22**, 1085 (1989).
- [48] A. Billoire, L. A. Fernandez, A. Maiorano, E. Marinari, V. Martin-Mayor, and D. Yllanes, *Finite-size scaling analysis of the distributions of pseudo-critical temperatures in spin glasses*, J. Stat. Mech. P10019 (2011).
- [49] M. Castellana, A. Decelle, and E. Zarinelli, *Extreme Value Statistics Distributions in Spin Glasses*, Phys. Rev. Lett. **107**, 275701 (2011).
- [50] A. J. Bray and S. A. Roberts, *Renormalisation-group approach to the spin glass transition in finite magnetic field*, J. Phys. C **13**, 5405 (1980).
- [51] A. J. Bray and M. A. Moore, *Evidence for massless modes in the ‘solvable model’ of a spin glass*, J. Phys. C **12**, L441 (1979).
- [52] A. Sharma and A. P. Young, *de Almeida-Thouless line in vector spin glasses*, Phys. Rev. E **81**, 061115 (2010).
- [53] C. de Dominicis, I. Giardinà, E. Marinari, O. C. Martin, and F. Zuliani, *Spatial correlation functions in three-dimensional Ising spin glasses*, Phys. Rev. B **72**, 014443 (2005).
- [54] D. J. Thouless, J. R. L. de Almeida, and J. M. Kosterlitz, *Stability and susceptibility in Parisi’s solution of a spin glass model*, J. Phys. C **13**, 3271 (1980).
- [55] Y. Imry and S.-K. Ma, *Random-Field Instability of the Ordered State of Continuous Symmetry*, Phys. Rev. Lett. **35**, 1399 (1975).
- [56] J. Yeo and M. A. Moore, *Critical point scaling of Ising spin glasses in a magnetic field*, Phys. Rev. B **91**, 104432 (2015).
- [57] M. A. Moore, *1/m expansion in spin glasses and the de Almeida-Thouless line*, Phys. Rev. E **86**, 031114 (2012).
- [58] URL <http://goo.gl/Dk94G0>.
- [59] G. Parisi and T. Temesvári, *Replica symmetry breaking in and around six dimensions*, Nuc. Phys. B **858**, 293 (2012).